# Na double-edge magneto-optic filter for Na lidar profiling of wind and temperature in the lower atmosphere

**Wentao Huang,[1] Xinzhao Chu,[1,*] B. P. Williams,[2] S. D. Harrell,[3] Johannes Wiig,[1] and C.-Y. She[3]**

[1]*University of Colorado at Boulder, 216 UCB, CIRES, Boulder, Colorado 80309, USA*
[2]*NWRA Colorado Research Associates, 3380 Mitchell Lane, Boulder, Colorado 80301, USA*
[3]*Colorado State University, Fort Collins, Colorado 80523, USA*
[*]*Corresponding author: Xinzhao.Chu@Colorado.edu*

Received September 26, 2008; accepted November 30, 2008;
posted December 12, 2008 (Doc. ID 102066); published January 14, 2009

A Na double-edge magneto-optic filter is proposed for incorporation into the receiver of a three-frequency Na Doppler lidar to extend its wind and temperature measurements into the lower atmosphere. Two prototypes based on cold- and hot-cell designs were constructed and tested with laser scanning and quantum mechanics modeling. The hot-cell filter exhibits superior performances over the cold-cell filter containing buffer gas. Lidar simulations, metrics, and error analyses show that simultaneous wind and temperature measurements are feasible in the altitude range of 20–50 km using the hot-cell filter and reasonable Na lidar parameters. © 2009 Optical Society of America

*OCIS codes:* 280.3640, 300.6210, 010.3640.

Resonance fluorescence Na Doppler lidars measure wind and temperature simultaneously in the mesosphere and lower thermosphere [1]. They have made significant contributions to the study of atmospheric wave dynamics. Unfortunately, their measurements are limited to 80–105 km where the trace gas Na atoms are available. Wave coupling studies require simultaneous profiling of wind and temperature from the lower to the upper atmosphere. It is therefore desirable to extend the Na lidar measurements into the lower atmosphere. Such capability can be achieved in principle by the Rayleigh Doppler lidar techniques. Fabry–Perot interferometers (FPIs) and iodine filters have been proposed and evaluated [2–5].

In this Letter, we propose a Na magneto-optic filter to function as a double-edge filter in the receiver of a three-frequency Na Doppler lidar to extend its wind and temperature measurement range into the lower atmosphere. The idea was initially proposed by one of the authors (Williams), originating from the Na magneto-optic filter in solar observations [6] and the mesopause magneto-optic Doppler analyzer [7]. We name this filter the Na double-edge magneto-optic filter (Na-DEMOF). It has advantages over the FPIs and iodine filters because of its stable double-edge filter functions and the possibility of simultaneous profiling of wind, temperature, and aerosol when operated with a three-frequency Na Doppler lidar.

The Na-DEMOF setup is similar to the Faraday filter [8] used for Na lidar daytime observations: a Na vapor cell is placed within a longitudinal magnetic field B between two polarizers. The difference is a quarter-wave plate added between the Na cell and the second polarizer for the Na-DEMOF [see Fig. 1(a)]. Despite the similarity in the setup, the Faraday filter and the Na-DEMOF use different aspects of the Na resonance—the anomalous dispersion for the former and the absorption for the latter. The Na-DEMOF is solely based on the different Na absorptions to circularly polarized light under the influence of a magnetic field and then followed by polarization analysis with a quarter-wave plate and a polarized beam splitter. The static magnetic field across the Na cell causes the Zeeman splitting of Na energy levels, which shifts the resonance frequencies for the left- and right-circularly polarized light down and up, respectively, from the zero-field resonance. A medium-strength magnetic field is used in the Na-DEMOF to yield certain absorption at the signal frequencies. The Na absorptions for two circular polarizations are shown as the dashed and dotted–dashed curves in Fig. 1(b). The crossed edges near the zero frequency offset form the double edges required by a double-edge filter. The lidar return light scattered from atmospheric molecules and aerosols passes through the first polarizer becoming linearly polarized. It can be decomposed into two circular polarizations with

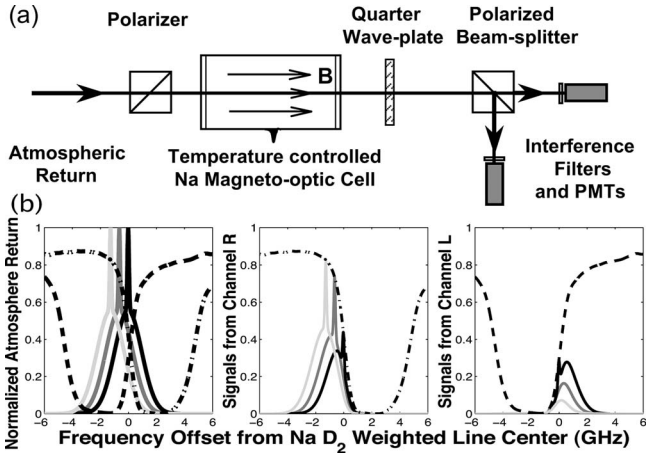


Fig. 1. (a) Na-DEMOF setup. (b) Measured left-channel (dashed curve) and right-channel (dotted–dashed curve) edge filter functions. Solid curves represent simulated atmospheric returns from the Na lidar three frequencies (left panel) and filter output (middle and right panels).

 

equal amplitudes. Owing to the different absorptions experienced by the two circular polarizations in the Na vapor cell under a longitudinal magnetic field, the light exiting the Na cell consists of two circularly polarized components with different intensities [Fig. 1(b)]. A quarter-wave plate converts them into two linear polarizations that are perpendicular to each other and symmetric about the axis of the quarter-wave plate with a 45° off-axis angle. The polarized beam splitter following the wave plate separates the two linear polarizations into two channels for photon detection. The intensity ratio between the two channels is a sensitive function of Doppler frequency shift, Doppler broadening, and aerosol loading. The three-frequency Na Doppler lidar [1] provides three independent ratios. In this way, the Na-DEMOF acts as a double-edge filter, enabling wind and temperature profiling from pure molecular scattering in the lower atmospheric region free of aerosols. When aerosols are present even lower in the atmosphere, the three unknown parameters (wind, temperature, and aerosol backscatter ratio) can be derived, in principle, from the three independent ratios. To accurately separate the two circular polarizations, the wave plate must be an exact quarter-wave plate at the desired wavelength, and the transmission orientation of the polarized beam splitter must be set exactly 45° relative to the quarter-wave plate axis. The input polarizer orientation is not important and can be rotated to maximize the signal transmission.

Based on above principles we constructed and laboratory-tested two prototypes of the Na-DEMOF. The cold-cell prototype has the same design as in [7]. Its Na vapor cell is 9 cm long and filled with ~20 mbar argon buffer gas. Only the Na reservoirs are heated, and the buffer gas is used to confine the Na vapor near the center to prevent Na coating the windows. The hot-cell filter uses a shorter cell (5 cm) without any buffer gas. The entire cell is heated to a desired temperature with ±0.1°C precision. The magnetic fields in the center of the cells are ~1400 and 1500 G for the cold- and hot-cell filters, respectively. The filter functions were measured with a Coherent 899-21 ring dye laser by scanning the laser frequency in a range of ±12 GHz around the Na $D_{2a}$ peak (589.15826 nm). The absolute frequency was derived from the Doppler-free saturation-absorption spectroscopy taken simultaneously from a reference Na vapor cell. Only 10 $\mu$W of ring dye laser power was used as the input signals to the filter to avoid saturation. The fluctuation of input laser power was monitored simultaneously and corrected. Figure 2 illustrates filter functions measured at different temperatures, which were normalized to the transmitted power of each channel without the Na cell, excluding the loss from the polarizers and the quarter-wave plate. The hot-cell filter has much higher out-of-band transmission than that of the cold-cell prototype. The large signal loss in the cold-cell is attributed to the contaminated windows of the aged cell. The slopes of the absorption edges are steep for the hot-cell filter. The transmission rises from minimum to maximum within ~3 GHz, in contrast to the slow slopes

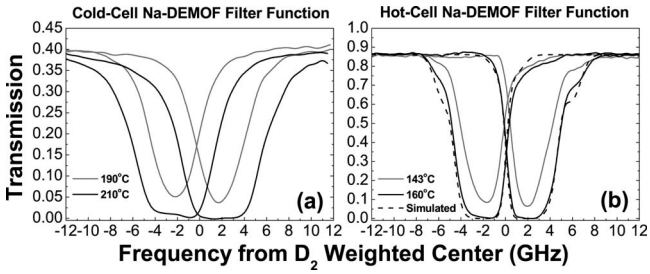


Fig. 2. Measured filter functions at different temperatures: the reservoir temperatures for the cold-cell and the window temperatures for the hot-cell. The dashed curves in (b) are QM simulated hot-cell filter functions at 160°C and 1350 G.

(~7 GHz) for the cold-cell filter. Given the FWHM of the Doppler broadened Rayleigh scattering is 2.3 GHz at ~280 K, the steep edge provides much better signal transmission, which substantially helps reduce the measurement errors caused by the photon noise. Thus, the hot-cell Na-DEMOF exhibits superior performances over the cold-cell filter.

We successfully modeled the measured hot-cell filter functions with quantum mechanics (QM) calculations [see Fig. 2(b)]. The QM code was adapted and modified from a Faraday filter computation developed by Harrell *et al.* [9]. The difference between the measured and the simulated magnetic field strengths is likely caused by the calibration of the Gaussmeter used. With a uniform Na density in the hot-cell, the inhomogeneity of the magnetic field is not critical for the slopes of the filter edges. Our calculation shows stronger dependence of the filter shape on the temperature (i.e., Na density) but much weaker dependence on the magnetic field. For the cold-cell filter functions, although the QM code can generate the stretched slopes up to ~4.5 GHz when considering the inhomogeneity of the Na density and magnetic field, it is not possible to reproduce the observed slopes. This is likely due to the pressure broadening caused by the buffer gas, which is not considered in the QM code.

We search the best ratio metrics for wind and temperature measurements in lower atmosphere when such a hot-cell Na-DEMOF is implemented in the receiver of a three-frequency Na Doppler lidar [1]. In the lower atmospheric region free of aerosols, the lidar returns consist of pure Rayleigh scattering by air molecules, which is Doppler broadened. Its width varies with the temperature, and its central frequency shifts with the line of sight (LOS) wind. A Na Doppler lidar runs three frequencies consecutively at $f_a = -651.4$ MHz and $f_\pm = f_a \pm 630$ MHz relative to the Na $D_2$ line center [1]. The lidar returns at each frequency are split into two channels corresponding to the left- and right-circular polarizations, respectively. Thus, we have six signal channels from three frequencies. Changes in wind or temperature cause changes in the ratios between the left and right channels. Our metrics search is to determine the ratios that are highly sensitive to temperature or wind changes while allowing highest possible signal transmittance and possessing minimum cross talk. These

factors lead to minimum measurement errors. Based on the Na lidar operating frequencies and the measured hot-cell filter functions at 160°C, the best wind and temperature metrics are found to be

$$R_W(V_{\mathrm{LOS}},T)=\frac{N_{R+}-N_{L+}}{N_{R+}+N_{L+}},$$

$$R_T(V_{\mathrm{LOS}},T)=\frac{N_{L-}}{N_{R-}}, \tag{1}$$

where $V_{\mathrm{LOS}}$ is the line of sight wind, $T$ is the temperature, and $N$ is the photon count from different frequencies and channels. The subscripts $L$ and $R$ represent the left and right channels, while + and − denote the operating frequencies $f_+$ and $f_-$. Figure 3 shows the sensitive dependence of these two ratios on LOS wind and temperature.

Utilizing an error analysis approach similar to that described in [1], we derive the measurement uncertainties caused by photon noise under nighttime conditions (nearly zero background light) in Eq. (2),

$$(\Delta V_{\mathrm{LOS}})_{\mathrm{rms}}=\frac{1}{\partial R_W/\partial V_{\mathrm{LOS}}}\frac{(1+R_W)\sqrt{(1-R_W)/2}}{\mathrm{SNR}_{R+}},$$

$$(\Delta T)_{\mathrm{rms}}=\frac{1}{\partial R_T/\partial T}\frac{\sqrt{(1+R_T)R_T}}{\mathrm{SNR}_{R-}}, \tag{2}$$

where the signal-to-noise ratios are defined as $\mathrm{SNR}_{R\pm}=N_{R\pm}/\Delta N_{R\pm}$. Adopting a lidar transmitter with 20 mJ per pulse energy at 50 Hz repetition rate and off-zenith angle $\theta=30°$, and a lidar receiver with 1 m telescope, 30% optical efficiency, and photomultiplier tube with 40% quantum efficiency at 589 nm, we performed a range-resolved lidar simulation of expected photon count profiles. The horizontal wind uncertainty $\Delta V_H=\Delta V_{\mathrm{LOS}}/\sin\theta$ and temperature uncertainty $\Delta T$ were derived using Eq. (2), and the results are shown in Fig. 4.

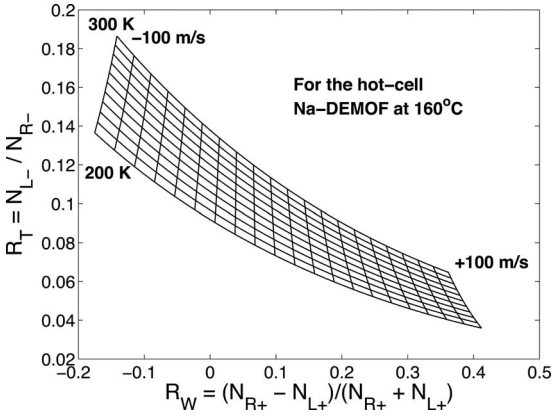


Fig. 3. LOS wind and temperature calibration curves.

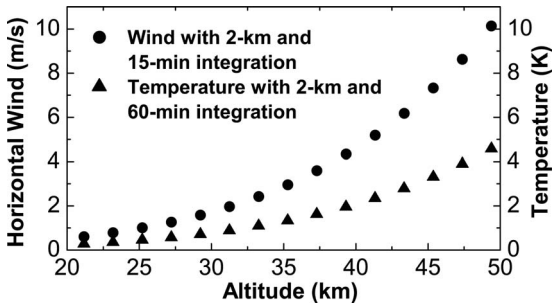


Fig. 4. Simulated measurement uncertainties due to photon noise using the hot-cell filter functions at 160°C.

In conclusion, it is feasible to simultaneously measure wind and temperature in the region of 20–50 km with the hot-cell Na-DEMOF implemented in the receiver of a three-frequency Na Doppler lidar. To further extend the measurements below 20 km, the aerosol influence must be taken into account. Three independent ratios derived from three frequencies must be used to derive the aerosol, wind, and temperature by an iteration approach. Below ~10 km where the atmospheric pressure is high, it is necessary to consider the Rayleigh–Brillouin scattering instead of the pure Rayleigh scattering [10]. Around the boundary layer where aerosol scattering is dominant, wind alone could be derived from aerosol scattering. As the last remark, a potassium-DEMOF using the similar principles proposed can be developed to extend K Doppler lidar measurements into the lower atmosphere.

This research is supported by the CIRES Innovative Research Program, National Science Foundation (NSF) grants CRRL ATM-0545353, ATM-0545262, and ATM-0545221, NSF CAREER ATM-0645584, and NSF MRI ATM-0723229.

## References

1. X. Chu and G. C. Papen, *Laser Remote Sensing*, T. Fujii and T. Fukuchi, eds. (CRC, 2005), pp. 179–432.
2. C. L. Korb, B. M. Gentry, and C. Y. Weng, Appl. Opt. **31**, 4202 (1992).
3. M. L. Chanin, A. Hauchecorne, A. Garnier, and D. Nedeljkovic, J. Atmos. Terr. Phys. **56**, 1073 (1994).
4. C. Flesia and C. L. Korb, Appl. Opt. **38**, 432 (1999).
5. C. Y. She, J. Yue, Z. Yan, J. W. Hair, J. Guo, S. Wu, and Z. Liu, Appl. Opt. **46**, 4434 (2007).
6. G. Agnelli, A. Cacciani, and M. Fofi, Sol. Phys. **44**, 509 (1975).
7. B. P. Williams, and S. Tomczyk, Appl. Opt. **35**, 6494 (1996).
8. H. Chen, C. Y. She, P. Searcy, and E. Korevaar, Opt. Lett. **18**, 1019 (1993).
9. S. D. Harrell, C.-Y. She, T. Yuan, D. A. Krueger, H. Chen, S. S. Chen, and Z. L. Hu, "Sodium and potassium vapor Faraday filters re-visited: Theory and applications," (submitted to J. Opt. Soc. Am. B).
10. G. Tenti, C. D. Boley, and R. C. Desai, Can. J. Phys. **52**, 285 (1974).